JOURNAL OF MATERIALS SCIENCE 16 (1981) 3059–3066

Fracture energy and surface topology in the cracking of high performance sulphone polymers

ROBERT Y. TING*
Polymeric Materials Branch, Chemistry Division, Naval Research Laboratory, Washington, DC 20375, USA

The dynamic mechanical properties and the fracture behaviour of three sulphone polymers that offer high temperature capability have been studied. Torsion pendulum analysis was performed over the temperature range − 150 to 225° C. Fracture tests were carried out using compact tension specimens and standard Izod impact specimens. It was found that the incorporation of additional groups in the backbone of the sulphone polymer introduced additonal low-temperature relaxation peaks in the dynamic mechanical loss curve and improved polymer fracture energy. The fracture energy of the sulphone polymers was also found to decrease as the loading rate was increased during fracture. The results of post-failure fractography are discussed.

1. Introduction

Fibre-reinforced organic composite systems exhibit superior specific modulus and tensile strength, and therefore have received considerable attention for potential aerospace and advanced ship applications. The thrust behind this trend is the possibility of replacing many metallic components with composite parts for weight reduction and hence energy saving. One good example is the application of composite materials in the vertical or short take-off and landing (V/STOL) aircraft. For such advanced applications conventional polymeric matrix materials such as polyesters and epoxies are not suitable since they have maximum use temperatures of only 90 to 120° C. Recently, many "high performance polymers", which offer 170 to 260° C temperature capability, have become available. These include tetrafunctional epoxies, thermosetting polyimides and some thermoplastic polymers such as polysulphone.

Thermoplastic sulphone polymers have recently been considered for composite matrix applications [1] and as potential structural adhesives [2, 3]. In these applications, failure is mainly governed by flaw growth and subsequent crack propagation. One of the important mechanical properties that needs to be evaluated for these polymers is therefore their resistance to crack propagation. Bascom *et al.* [4] recently determined the fracture energy of many high performance polymers and concluded that the thermoplastics are much "tougher" than the thermosetting materials. While this would certainly be translated into superior impact behaviour, the thermoplastics are also attractive because they can be formed easily and possess good storage and handling properties at room temperatures.

In this paper, the fracture behaviour of three high performance sulphone polymers will be reported together with their dynamic mechanical properties, as determined from a torsional pendulum analysis. Furthermore, fractographic work was carried out in the hope of obtaining additional information on the deformation involved in crack growth and propagation.

2. Experimental procedure

2.1. Materials

Three sulphone polymers were studied. Poly-

*Present address: Code 5975, Naval Research Laboratory, Orlando, FL 32856, USA.

0022–2461/81/113059–8$02.80/0

TABLE I Structures of sulphone polymers

Polymer	Trade name	Manufacturer	Structure
Polysulphone	Udel	Union Carbide	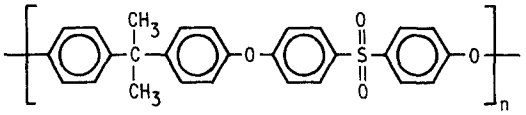
Polyphenylsulphone	Radel	Union Carbide	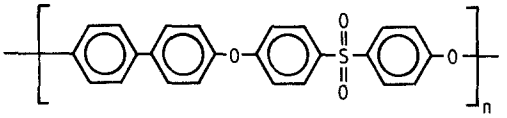
Polyethersulphone	Victrex	ICI America	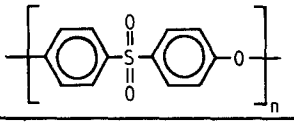

sulphone (Udel, abbreviated as PSF) and polyphenylsulphone (Radel, abbreviated as PPSF) samples were obtained from the Union Carbide Company. Polyethersulphone (Victrex, abbreviated as PESF) samples were supplied by ICI America, Inc. The chemical structures of these polymers are shown in Table I.

Plates of various thicknesses produced by the manufacturers were used as-received for preparing test specimens. Prior to testing, all specimens were treated according to the manufacturer-recommended annealing cycles to remove the "thermal skin" effect resulting from the moulding or extrusion process.

2.2. Torsional pendulum analysis (TPA)

Dynamic mechanical properties were determined by using a freely oscillating torsional pendulum [5] operating at about 1 Hz. The experiments were carried out in a nitrogen atmosphere in accordance with the recommended ASTM procedure, D-2236-70. The sample size was 10 cm x 1.25 cm x 0.075 cm. The frequency of the freely-damped wave and the logarithmic decrement $\Delta = \ln (A_i/A_{i+1})$, where A_i was the amplitude of the ith oscillation of the wave, were directly measured as the sample was heated from -150 to about 225° C at a rate of 1° C min^{-1}. These parameters led to the determination of the dynamic shear modulus and the loss factor of the sample as a function of temperature.

2.3. Fracture evaluation

Based on linear elastic fracture mechanics, the displacement l in the direction of a load P is

$$l = CP, \tag{1}$$

where C is the compliance of the specimen. Under a fixed load condition, any change in l may be related to a change in the crack length, a, by

$$\delta l = P\frac{dC}{da}\delta a. \tag{2}$$

The strain energy is $\epsilon = 1/2P\delta l$, which defines the strain energy release rate, or fracture energy, G

$$\epsilon = 1/2P\delta l = Gb \cdot \delta a, \tag{3}$$

where b is the specimen thickness. From Equations 2 and 3, one finds

$$G = \frac{P^2}{2b}\frac{dC}{da}. \tag{4}$$

Once dC/da is determined for a specific specimen geometry, a proper expression for G may be obtained to directly relate it to the load P and specimen dimensional parameters.

Polymer fracture energy was determined by using standard one-inch compact tension specimens [6] according to the ASTM procedure E-399-78. A precrack was introduced with a razor blade at the end of the saw-cut. Specimens were then fractured in an Instron testing machine at various cross-head speeds in order to determine polymer fracture energy at different loading rates. By measuring the critical failure load, P_c, one may calculate polymer fracture energy by Equation 4, which in this case becomes

$$G_c = Y^2P_c^2a/EW^2b^2, \tag{5}$$

where Y is a geometrical factor given by

$$Y = 29.6 - 186(a/W) + 656(a/W)^2 - 1017(a/W)^3 + 639(a/W)^4$$

and a is the crack length, E is the Young's modulus, W is the specimen width in the direction of the crack and b is the thickness [7]. The applicability of this equation is normally limited to the range of $0.3 \leqslant a/W \leqslant 0.7$.

Standard Izod impact tests were carried out using a Tinius-Olsen impact tester for plastics. The impact load and energy were recorded as a function of impact time. Based on the results of a linear elastic fracture mechanics analysis, the impact strength, ϵ, is shown to be related to the fracture energy [8] by combining Equations 3 and 4

$$\epsilon = G_c \phi b W. \tag{6}$$

The dimensionless factor ϕ is related to the specimen compliance, C, and its variation with respect to the crack length, a, such that

$$\phi = \frac{C_{(a)}}{\left[\frac{dC_{(a)}}{d(a/W)}\right]}. \tag{7}$$

This factor has been calculated and given in a tabulated form by Plati and Williams [9] for a standard Izod impact specimen. For the specimens used in this work, the length to width ratio was $2L/W = 5$ such that the factor ϕ may be plotted as a function of (a/W) as shown in Fig. 1. Once the impact energy ϵ is measured for specimens of various initial crack lengths, one may determine the fracture energy G_c by using Equation 6.

It should be noted that a standard Izod specimen has a blunt 45° notch. Careful precracking has been carried out using a razor-blade to initiate a starting crack approximately 0.05 cm in depth, (see Fig. 2). This practice has proven to be very useful in reducing the scatter of impact data. The technique of deriving fracture energy from impact data based on Equation 6 was validated by using a polymethylmethacrylate (PMMA) sample. The result, as seen in Fig. 3, indeed shows a linear relationship between the impact energy and the quantity $\phi b W$, passing through the origin if the impact energy is properly corrected for kinetic energy considerations [9]. The slope of the plot gives a fracture energy for PMMA of 1.82 kJ m^{-2}, which agrees very well with that obtained by others [9, 10].

3. Results and discussion

Fig. 4 shows the results for the three sulphone polymers. All samples exhibited very high dynamic shear modulus, of about 10^9 N m^{-2}. This high modulus value was maintained throughout the glassy region until the temperature approached the glass-to-rubber transition, where the modulus decreased

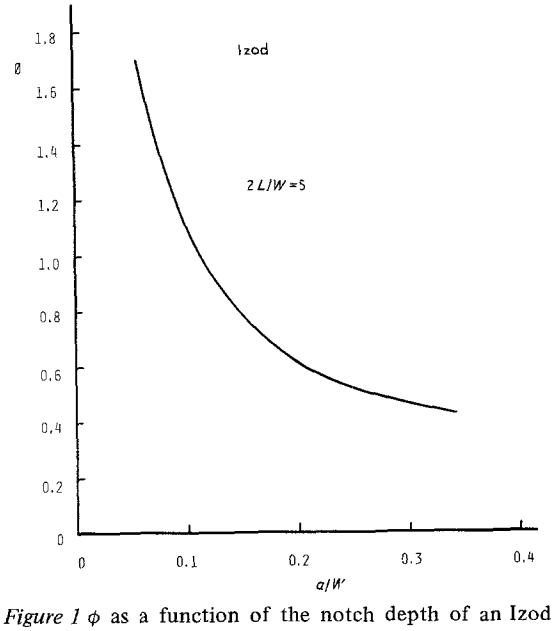

Figure 1 ϕ as a function of the notch depth of an Izod impact specimen.

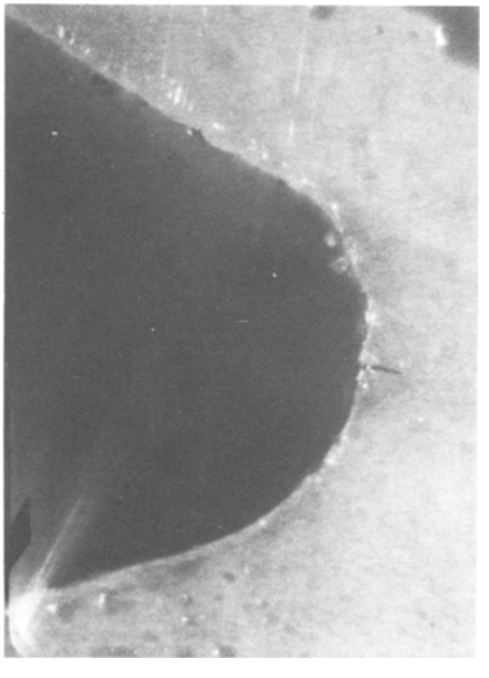

Figure 2 The precrack at the bottom of the 45° notch of an Izod impact specimen.

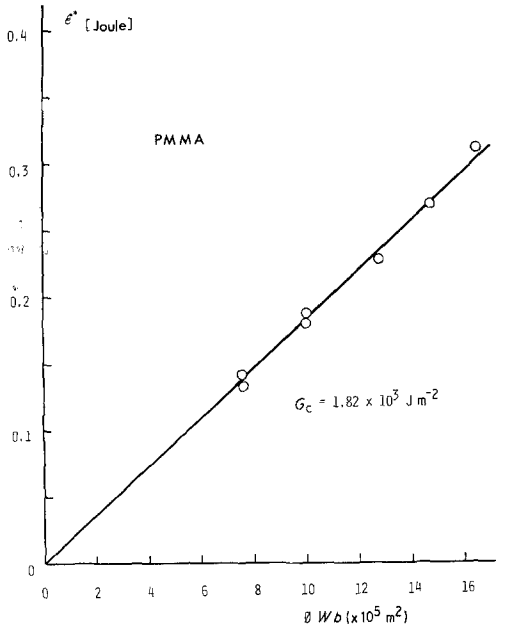

Figure 3 Linear plot of impact energy of PMMA against specimen geometrical parameters for the derivation of fracture energy.

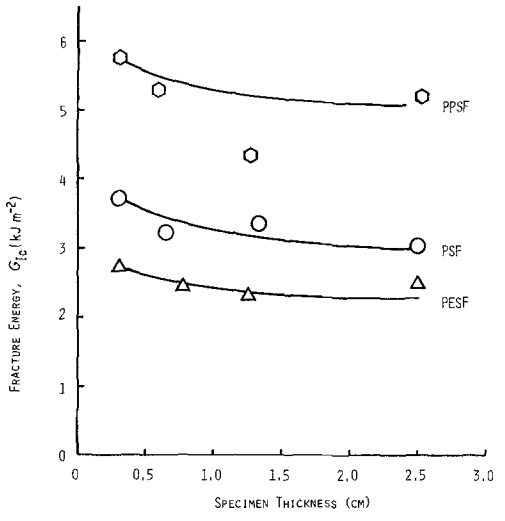

Figure 5 Dependence of specimen thickness on the fracture energies of sulphone polymers.

very rapidly with increasing temperature. The observed difference in modulus among the three polymers was very small. In terms of the loss factor Δ, the polymers had a common secondary relaxation peak at -90° C with a value of about 0.1. However, two major differences exist in the response of the polymers to small-amplitude oscillatory deformation. First, the glass-to-rubber transition temperature, T_g, where a sharp increase in Δ was coupled with a rapid decrease in modulus, was found to be the highest for PPSF (210° C), followed by PESF (203° C) then PSF (174° C). Second, in addition to the loss peak at -90° C, PSF exhibited another relaxation peak at about -20° C. For the PPSF sample a new broad peak was also found at about 100° C. These peaks suggested possible additional loss mechanisms in PSF and PPSF for energy absorption. The detail of these mechanisms is not yet known at the present time, but clearly the differences in the mechanical loss behaviour are related to the differences in molecular structure. The additional aliphatic group in bisphenol-A units of PSF or aromatic groups in

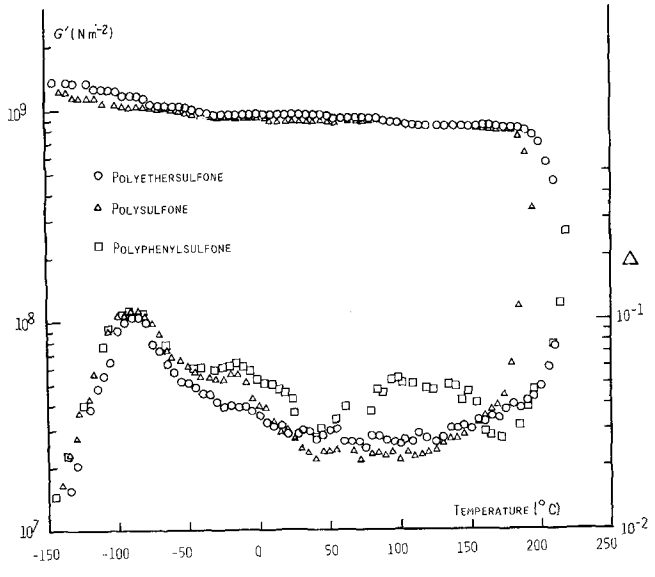

Figure 4 Torsional pendulum analysis result for sulphone polymers.

the backbone of PPSF could allow for new rotational mobility but become restraints leading to a decrease in molecular flexibility. The result could be very different packing configurations in PSF and PPSF compared with PESF, which has bisphenol-S groups as the repeating backbone units.

While keeping the Instron cross-head at a constant speed of 0.125 cm min^{-1}, the effect of sample thickness on the fracture energy of the sulphone polymers was determined using compact tension specimens with thicknesses ranging from 0.3 to 2.5 cm. Fig. 5 shows this specimen thickness dependence of polymer fracture energy. The data indicate that the measured fracture energy values indeed decrease gradually as sample thickness increases, except for the 1.25 cm polyphenylsulphone specimens. This abnormality may have its origin in the specific sample plate received from the manufacturer. The fracture energies level-off to constant values for specimens thicker than 1 cm. These constant values may therefore be taken as the plane strain G_c. In the case of polysulphone, the value of 3.1 kJ m^{-2} is in good agreement with that of 3.2 kJ m^{-2} reported by Gales and Mills [11].

The issue of plane stress versus plane strain for fracture failure is important in engineering design. The fracture energy based on plane stress is higher than that of plane strain [6]. The contribution of plane stress to fracture failure, relative to plane strain, increases with decreasing specimen thickness. By using the plane stress value, therefore, one could be overestimating the toughness of the material. In fact, in many structural components fracture tends to initiate from flaws such as surface scratches or from internal cracks, which, under stress, are subjected to essentially plane strain conditions. Therefore, the appropriate design criterion should be based on the plane-strain fracture energy.

It has been suggested [12] that for satisfactory plane-strain fracture toughness testing the specimen thickness should be greater than

$$b \geqslant \frac{2.5 G_c E}{\sigma_0^2}, \qquad (8)$$

where σ_0 is the yield strength of the material. The minimum thickness required for each polymer sample, calculated based on this criterion, is given in Table II, where the Young's modulus E was determined using the standard tensile test with the Instron cross-head moving at a speed of 0.125 cm min^{-1}. These results agree very well with the experimental observation in Fig. 5. Thus, for the sulphone polymers, one would readily satisfy the requirements for plane strain testing if 1 cm thick specimens were used.

Fig. 6 shows polymer fracture energy as a function of loading rate at room temperature. Since the actual strain rate based on the local deformation pattern or stress distribution at the crack tip is not known, the inverse of fracture time is used for the abscissa of Fig. 6. Only PSF and PESF were evaluated in this phase of the programme since PPSF was no longer available from the manufacturer. Both PSF and PESF polymers exhibited very high fracture energy: at lower loading rates the G_c values are of the order of 3 kJ m^{-2} in contrast with the values of about 0.1 kJ m^{-2} for many epoxies [4]. This high fracture energy may be attributed to the large free volume in amorphous glassy polymers as opposed to that in highly cross-linked epoxy systems. PSF fracture energy is approximately 25% higher than that of PESF at these low loading rates (10^{-3} sec^{-1}). Although the exact cause for this difference is still unclear at this moment, it is speculated that it is related to the differences in the dynamic mechanical properties of these polymers as observed in the TPA data. Various correlations between bulk mechanical properties, such as impact strength and yield strength, and secondary relaxation loss peaks have been observed and reported for glassy polymers [13]. At the moment it is generally accepted that small-scale segmental motions of polymer chains are responsible for the secondary relaxation processes, which are identifiable by the appearance of loss peaks in a dynamic mechanical measurement [14]. But the detailed mechanisms involved in relating such molecular motions to polymer bulk properties are not at all clear. The TPA results

TABLE II Minimum specimen thickness required for plane strain testing of sulphone polymers

Parameter	Polyphenylsulphone	Polysulphone	Polyethersulphone
E (GPa)	2.49	3.15	3.4
G_{Ic} (kJ m^{-2})	5.5	3.1	2.6
σ_0 (MPa)	71.7	70.4	84.2
b_{min} (cm)	0.64	0.49	0.26

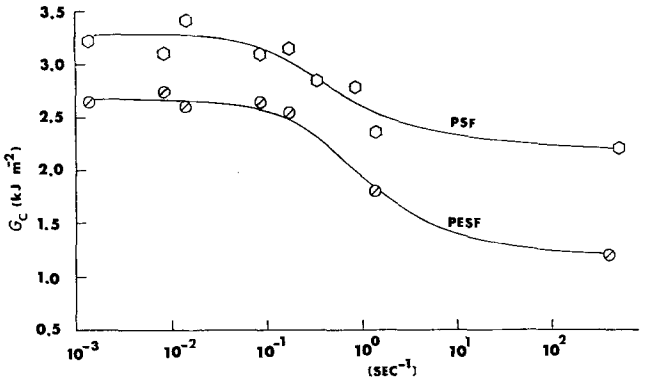

Figure 6 Effect of loading rate on the fracture energy of sulphone polymers.

obtained at about 1 Hz (Fig. 4) showed a loss peak at $-20°$ C for PSF, which was not found in PESF. This seems to suggest an additional loss mechanism in PSF for energy absorption. As indicated earlier, the bulky bisphenol-A groups may introduce steric hindrance and cause the PSF molecules to be less flexible. It therefore results in a different molecular packing and gives more free volume to PSF than PESF for resisting crack initiation and propagation in their amorphous glassy states because of the differences in polymer backbone structure. A detailed study on molecular motions in glassy sulphone polymers is currently under way at this laboratory.

The higher fracture energy PSF exhibited over PESF is amplified at higher loading rates. With increasing loading rate, both polymers showed a very rapid decrease in fracture energy. It should be pointed out, in the calculation of fracture energy G_c by using Equation 5, the low rate values of E given in Table II were applied. It may be reasonable to consider that the Young's modulus itself is also rate dependent. However, based on the time–temperature equivalence principle of polymer viscoelasticity [15], one may consider an increase in rate to correspond to a decrease in temperature. Fig. 4 shows that as the glassy state is approached the moduli of polymers remain practically constant. The effect of a slight increase in moduli at low temperature or high rate is that the decreasing trend of G_c with increasing rate shown in Fig. 6 would become slightly more pronounced. At very high loading rates, typically represented by the impact test results, the fracture energy eventually reaches a low, asymptotic value. The transition from high to low fracture toughness with increasing loading rate is centred around 0.5 sec^{-1}. In PESF this decrease in fracture energy is more pronounced than in PSF. At the highest rate tested, corresponding to the impact condition, PSF is shown to be approximately twice as tough as PESF.

4. Fractography

Post-failure analysis of the fracture surfaces was carried out using scanning electron microscopy

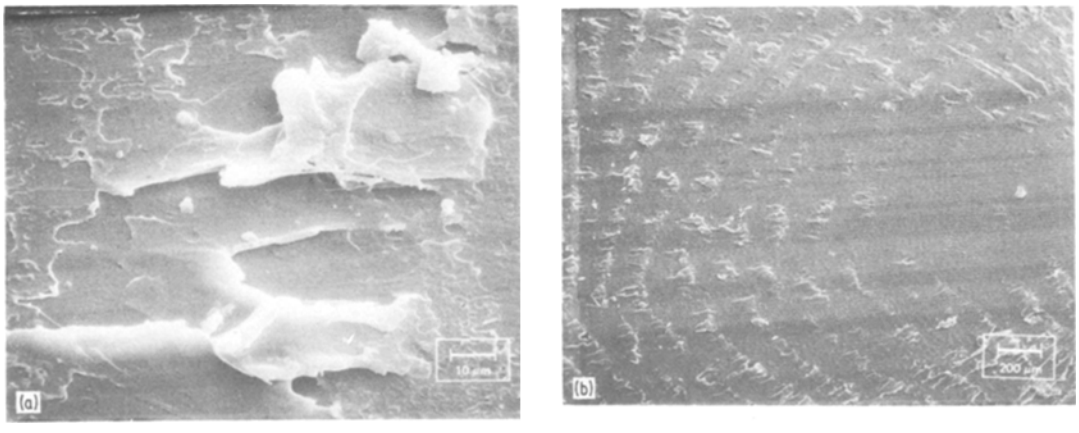

Figure 7 (a) and (b) SEM micrographs showing crack initiation in sulphone polymers. The crack propagates from right to left.

(SEM). Fig. 7. is a micrograph taken from a 1.25 cm thick specimen, showing the typical pattern of crack initiation from the precrack, which is to the immediate right of the picture. Initial crack extension seems to have been confined to the centre or the plane strain region. As the crack began to grow, a slow but unstable cracking zone was developed in which local plastic deformation was prominent. This process produced a surface topology containing concentric rings, which were also observed in other polymer systems and referred to as of the "Wallner-type" lines [16, 17]. The arc shape pattern suggests some type of crack-front stress-wave interaction. Smoley [16] related these ring structures to crack propagation through the craze which was induced by precracking and consisted of long elongated microvoids interconnected by stretched polymeric material in an opening-mode stress field. In the featureless areas, the crack tip went through the craze; in the rough areas, the crack tip spalled off uncrazed polymer to form these concentric rings. At higher magnification, the spalled-off region suggests intensive local tearing and yielding, whereas the smooth region shows signs that a porous microvoid structure existed before the crack front went through.

As the crack continued to propagate, the sporadic tearing marks eventually merged to form irregular river patterns along the direction of crack propagation, as seen in Fig. 8. These deep streaming tear marks, indicative of plastic deformation to a considerable depth below the surface, are coupled with the formation of long and highly extended filaments. Such fibrillar structures have also been observed in the fracture of polyvinyl chloride [16] and polycarbonate [18]. The formation of fibrils was suggested to be related to local adiabatic heating [18, 19] and plastic instability [20]. Apparently, as the crack progressed, the crack speed rapidly increased and local softening caused the material to be pulled out. The linear form of the fibrils with a tapered base and uniform diameters indicate that they were in tension and have been highly extended. They appear to have ruptured in a ductile manner and necked down to complete separation by shear deformation. Once ruptured, the fibrils generally fell onto the lower polymer surface and stuck there, further indication of the existence of a local adiabatic thermal condition. Overall, these characteristics of local shearing, the formation of a river pattern and fibrillar structure seemed to correlate with polymer toughness. For samples such as PSF that exhibited high fracture energies, these characteristics were noticeably more intense than those observed in PESF.

Finally, at distances further from the initiation zone, the fracture surface appeared shiny to the naked eye. Under SEM the surface topology of this fast cracking zone was typical for a brittle fracture in plastics, characterized by a relatively smooth appearance with the exception of few isolated parabolic markings. These markings have also been reported in the fractures of PMMA [21, 22] and polycarbonate [17], and are believed to be the result of interactions between the main and some localized, secondary crack fronts. Johnson and Radon [22] observed that in PMMA the secondary cracks originated from the cusps of the parabolic markings, where they often found small particles. In this study, particles have not been

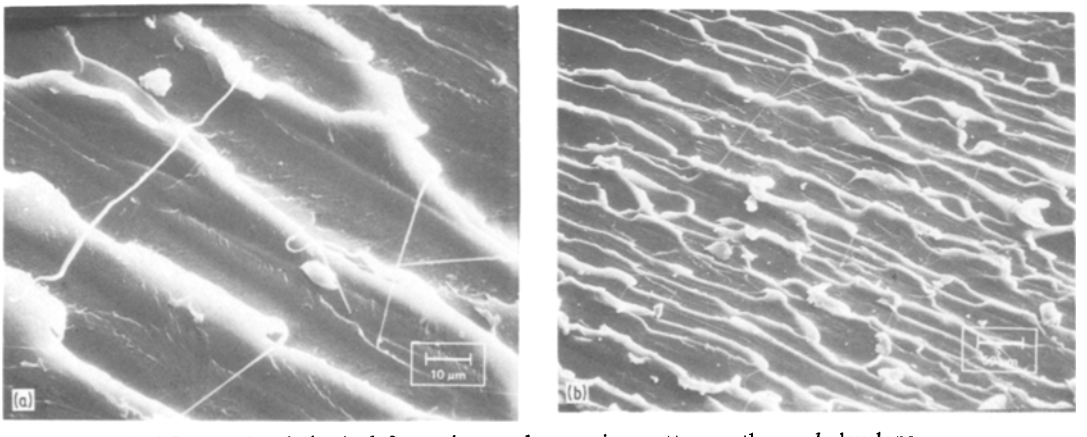

Figure 8 (a) and (b) Intense local plastic deformation produces a river pattern as the crack develops.

found in the sulphone polymers, a situation similar to that in polycarbonate [17].

5. Conclusions

Thermoplastic sulphone polymers were found to be much tougher than thermosetting epoxy polymers. Among the three polymer samples examined, polyphenylsulphone exhibited the highest fracture energy, followed by polysulphone and polyethersulphone. The differences are attributed to the effects of molecular structure and packing configuration. It was also shown that the fracture energy of sulphone polymers decreases rapidly with increasing loading rate. This suggests that the materials, if used for high rate applications such as impact, would not appear to be as tough as the fracture energy determined in a low rate experiment would indicate.

Post-failure morphological studies on fracture surfaces revealed that initial crack growth was confined to the plane strain region involving crack propagation through a craze zone. As the crack speed increased, intensive plastic deformation at the crack tip led to the development of a river pattern with the formation of fibrillar structures, indicative of a local adiabatic thermal condition. In the fast-crack area, secondary cracks were apparent which interacted with the main crack front to produce parabolic markings on the fracture surfaces of sulphone polymers.

References

1. G. E. HUSMAN and J. T. HARTNESS, *SAMPE Series* **24** (1979) 21.
2. S. G. HILL, E. E. HOUSE and J. T. HOGGATT, Boeing Aerospace Company Report D180-24744-1, (1978).
3. R. Y. TING and R. L. COTTINGTON, *SAMPE Series* **12** (1980) 714.
4. W. D. BASCOM, J. L. BITNER and R. L. COTTINGTON, *Amer. Chem. Soc., Org. Coat. Plast. Chem. Preprint* **38** (1978) 477.
5. L. E. NELSON, "Mechanical Properties of Polymers and Composites", Vol. 1 (Marcel Dekker, New York, 1974) p. 15.
6. J. F. KNOTT, "Fundamental of Fracture Mechanics" (Butterworths, London, 1973) p. 131.
7. W. SCHULTZ, in "Fracture Mechanics of Aircraft Structures", edited by M. Liebowitz, AGARDograph, AGARD Report AG-176 (NTIS, Springfield, VA, 1974) p. 37.
8. P. E. REED, in "Developments in Polymer Fracture", Vol. 1, edited by E. H. Andrews (Applied Science Pub., London, 1979) p. 121.
9. E. PLATI and J. G. WILLIAMS, *Polymer Eng. Sci.* **15** (1975) 470.
10. F. A. JOHNSON and J. C. RADON, *J. Eng. Fract. Mech.* 4 (1972) 555.
11. R. D. R. GALES and N. J. MILLS, *ibid.* **6** (1974) 93.
12. J. E. SRAWLEY and H. F. BROWN, Plane Strain Crack Toughness Testing, ASTM STP-410 (1966).
13. R. F. BOYER, *Polymer Eng. Sci.* 8 (1968) 161.
14. R. N. HAWARD, "The Physics of Glassy Polymers" (Halsted Press, John Wiley and Sons, New York, 1973) p. 198.
15. J. D. FERRY, "Viscoelastic Properties of Polymers", 2nd edn (John Wiley and Sons, New York, 1970) Ch. 11.
16. E. M. SMOLEY, in "Fracture Mechanics", edited by C. W. Smith, ASTM STP-667 (American Society for Testing and Materials, Philadelphia, PA, 1979) p. 700.
17. G. H. JACOBY, Fracture Surface and Process in Polycarbonate, ASTM STP-453 (1969).
18. A. CROSS and R. N. HAWARD, *J. Polymer Sci., Polymer Phys. Ed.* **11** (1973) 2423.
19. F. A. JOHNSON and J. C. RADON, *Materialprüfung* **15** (1973) 397.
20. J. M. KRAFFT and H. L. SMITH, NRL Memo Report 2598, Washington, DC (1973).
21. J. A. KIES, A. M. SULLIVAN and G. R. IRWIN, *J. Appl. Phys.* **21** (1950) 716.
22. F. A. JOHNSON and J. C. RADON, *Materialprüfung* **12** (1970) 307.

Received 23 January and accepted 9 April 1981.